AUTOGENEOUS SHRINKAGE OF MORTARS MADE WITH DIFFERENT TYPES OF SLAG CEMENT

Article *in* Transactions of the Japan Concrete Institute · July 2010

3 authors:

Januarti Jaya Ekaputri
Institut Teknologi Sepuluh Nopember

Tetsuya Ishida
The University of Tokyo

Koichi Maekawa
Yokohama National University

- Technical Paper -

AUTOGENEOUS SHRINKAGE OF MORTARS MADE WITH DIFFERENT TYPES OF SLAG CEMENT

Januarti Jaya EKAPUTRI[*1], Tetsuya ISHIDA[*2], Koichi MAEKAWA[*3]

ABSTRACT
The autogeneous shrinkage of mortars from seven slag-cements categorized as type B is presented. Specimens were cured under sealed condition at 20^{o}C and 50^{o}C with water to binder ratio of 35%. The experimental results showed higher shrinkage when BFS was introduced to OPC and a great scattered of shrinkage occurred at specimen from slag cement type B. Increase of curing temperature led to the great shrinkage at the first week. The slag content, fineness and chemical composition were thought to be the main factor of the shrinkage magnitude.
Keywords: autogeneous shrinkage, slag, mortar, embedded gauge

1. INTRODUCTION

Substitution of Blast furnace slag (BFS) for Portland cement is thought to have many advantages in generally such as good resistance to chloride ions attack, reduced heat of hydration and controlling alkali-aggregate reaction compared to normal Portland cement. BFS as a waste material, rich in SiO_2, and Al_2O_3 is produced in large quantities. At lower cost and lower environmental impact, per unit volume, its application can perform similar properties.

However, it was reported that autogenous shrinkage of concrete increases when cement contains BFS. This increase of autogeneous shrinkage is promoted by higher percentages of cement replacement by the slag and its application to low water to binder ratio [1]. Higher slag cement type B, specified in JIS R 5211 [2] is a general purpose blended cement containing 30% to 60% of slag. Some commercials-cements classified in slag cement type B have been found showing a great different in autogenous shrinkage [3].

The purpose of this paper is to investigate autogenous shrinkage of mortar using different slag cements which can be categorized in slag cement type B. In this study, specimens were prepared by mortar having 35% of W/C and adopted from 7 slag cements. Specimens were cured at sealed condition for 40 days under 20^{o}C and 50^{o}C of curing temperature and a constant relative humidity of 60%. Autogeneous shrinkage and internal RH change of each specimen were measured by embedded sensors. At the same condition, the results were then compared with the shrinkage of OPC mortar and the one made with 40% of BFS substitution in cement weight. Compressive strength obtained was then plotted to the shrinkage at a certain age.

Furthermore, by investigating the results, the authors discuss about influential factors to deal with shrinkage problems regarding the application of slag cement in the mixture.

2. TEST PROGRAMS

2.1 Materials

(1) Physical and chemical composition of cements

Seven slag cements from some sources were adopted in this study. Henceforth, these slag cements are coded as A, B, C, D, E, F, and G.

As a control system, pure ordinary Portland cement (OPC) with chemical composition as shown at Table 1 was use. Physical properties of OPC and slag cements are listed at Table 2. Some additional specimens were prepared containing 40% of cement weight partially replaced with BFS which has 4100cm^2/g of blaine surface area and 2.88g/cm^3 of density.

Table 3 shows mineral composition of cement. According to the data sheet of each material, mineral composition of OPC was determined by Bouge equation while Rietveld method was used for all slag cements. According to specification in JIS R 5211, slag cements A, B, C, D, E, F, and G can be categorized as slag cement type B as their slag content is in the aforementioned range. Among all materials, BFS content in slag cement G is the highest.

Tabel1 Chemical composition (%) of OPC

SiO_2	Al_2O_3	Fe_2O_3	CaO	MgO	SO_3	LOI
21.36	5.28	2.66	65.02	1.46	2.08	1.77

*1 PhD Student, Dept. of Civil Engineering, University of Tokyo, JCI Member
*2 Associate Prof., Dept. of Civil Engineering, University of Tokyo, JCI Member
*3 Prof., Dept. of Civil Engineering, University of Tokyo, JCI Member

Table 2 Physical properties of the cements.

Code	Density (g/cm^3)	Blaine surface area (cm2/g)	Ave Particle size (µm)	Particle width dist (N)
OPC	3.16	3480	n/a	n/a
A	3.06	4000	14.5	0.99
B	3.05	3630	16.8	1.08
C	3.02	3750	16.0	1.03
D	3.04	3880	13.7	0.97
E	3.04	4150	14.9	1.01
F	3.01	3790	15.9	0.98
G	2.98	3380	16.2	0.95

Table 3 Mineral and chemical composition

Code	Composition (%)										
	C_3S	C_2S	C_3A	C_4AF	Lime	MgO	Gyp	Hemi	Anhy	**Calcite**	**SO_3**
OPC	57.0	18.0	9.0	8.0	n/a	n/a	n/a	n/a	n/a	n/a	n/a
A	66.2	10.9	4.8	11.4	-	0.6	0.5	5.2	0.3	-	1.76
B	58.6	10.4	7.1	11.1	-	0.5	2.4	4.5	-	5.4	1.90
C	62.6	10.1	5.2	10.7	-	0.6	2.9	2.8	1.4	3.7	2.11
D	58.6	10.2	5.1	11.7	0.1	0.6	1.0	3.9	3.9	4.0	2.35
E	53.2	16.5	9.5	10.4	-	-	3.2	4.5	-	2.7	1.90
F	59.6	13.7	5.7	10.2	-	0.1	2.9	4.7	-	3.2	1.96
G	53.3	6.4	6.5	10.5	-	0.6	1.8	2.6	14.2	3.7	3.35

(2) Mix proportion of mortar

Mortar specimens having 35% of water to binder ratio were prepared with different mix proportions depending on density of slag cements shown in Table 4. In order to improve performance in fluidity of the fresh mortar, a superplasticizer from SP8SBS of 0.55% cement weight was used. Sand having density of $2.63g/cm^3$ was used as fine aggregate with 40% volume.

Table 4 Mix Proportion of Specimens (kg/m^3)

Code	Cement	Water	Sand	SP	BFS
OPC	846.27	296.19	988.9	4.65	0
A	833.34	291.67	988.9	4.58	0
B	832.02	291.21	988.9	4.58	0
C	828.04	289.81	988.9	4.55	0
D	830.70	290.74	988.9	4.57	0
E	830.70	290.74	988.9	4.57	0
F	826.71	289.35	988.9	4.55	0
G	822.67	287.94	988.9	4.52	0
OPC+BFS	507.76	296.19	988.9	4.65	338.5

2.2 Experimental Method

(1) Experimental setting

Mortar was cast in a cylindrical mold of 50 mm in diameter and 100 mm in length. A 0.2 mm thick polytetrafluoroethylene (Teflon) sheet was placed between the mold and the mortar in order to avoid restraint of deformation by the mold. In this study, the measurement of autogenous shrinkage was carried out by measuring the change in linear length of the specimen according to a method proposed by Nawa [4] as illustrated in Fig 1. The gauge was placed in the center of the mold and fix with a rubber. Immediately after the mortar was poured, the mold was then covered with paraffin film and wrapped with an aluminum tape to ensure the sealed condition. All specimens were kept in an environmental conditioned room at constant temperature of 20°C and 50°C and a constant relative `humidity of 60%. A thermocouple was also included in the gauges so the change in both internal temperature and strain were continuously measured and recorded. An average value from 3 specimens in the same condition and mixture was obtained.

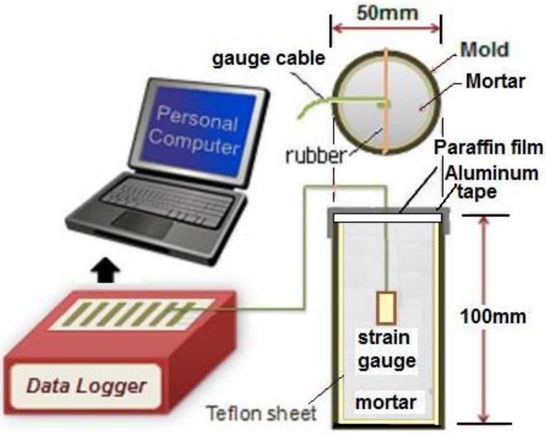

Fig 1 Autogeneous shrinkage measurement apparatus

(2) Strain gauge types

A 70 mm long thin pre-embedded strain gauge from Kyowa Dengyo, named KMC-70-120-H3 (type A) covered with waterproof silicone and 30mm in gage length of KM-30-120-H1-11 (type B) covered with acrylic were used. Fig 2 shows the gauges picture. Catalogue products released by the company inform that type A can be affected by the moisture conditions surrounding the gauges while type B provides suitable waterproof in mortar purposes. To eliminate this issue, the gauges need to be immersed in pure water before using.

Fig 2 Strain gauges type A (left) and B (right)

Measurement results to observe the influence of moisture can be seen in Fig 3. The gauges were soaked and dried in room temperature (20°C) with a constant RH of 60% alternately. It is clearly seen that gauge type B has a good resistant in moisture change while an abrupt decrease or increase of strain is shown by type A during wetting-drying at given time.

In this research, all the gauges were soaked for 2 weeks before casting and the strain change caused by water absorption of the air-dried gauge was observed until the strain reading was stable. Under normal temperature, both gauges plotted in Fig 4 give almost the same result. In room temperature, gauges type A were adopted while gauges type B were applied in higher temperature (50°C).

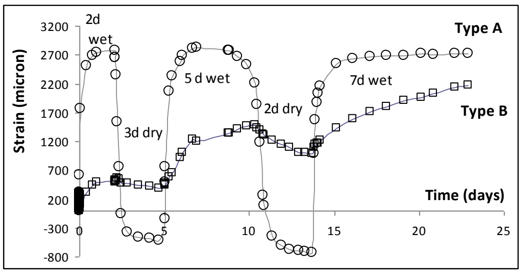

Fig 3 Expansion and shrinkage of gauges in water

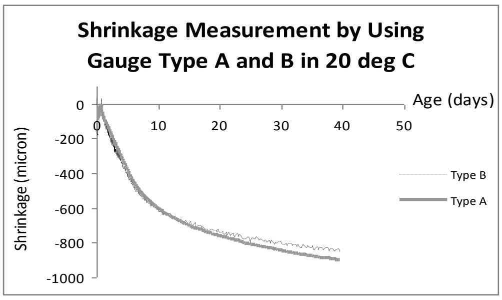

Fig 4 Comparison between two types of embedded gauge

(3) Reliability and reproducibility

At 20^{o}C of temperature and 60% of relative humidity, mechanical strain gauges (contact chip) were also used (Fig 5) for reliability result which is given in Fig 6. Comparatively, from three identical specimens, the difference in shrinkage between contact gauges and embedded gauges was only up to 40µ. Total weight loss due to evaporation subjected to aluminum lid during measurement was 0.1% at age 15 days.

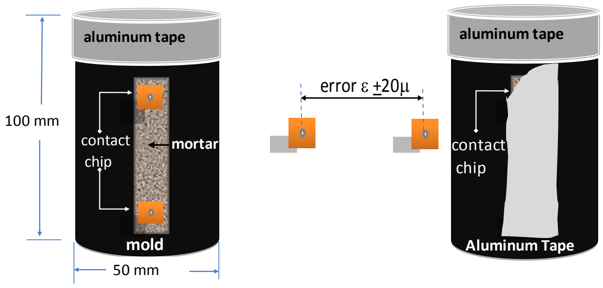

Fig 5 Shrinkage measurement with contact gauges

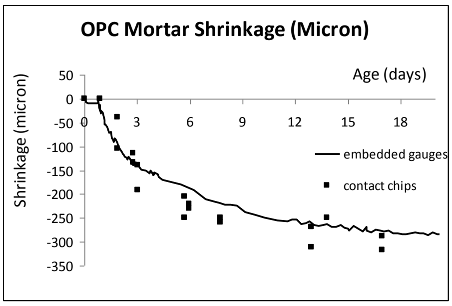

Fig 6 Comparison results of shrinkage between embedded and contact gauges

Fig 7 plots the shrinkage measurement against time curves for four parallel specimens with an identical mix proportion by using embedded gauges. The similarity of the four curves verifies that the measurement method has a good reproducibility.

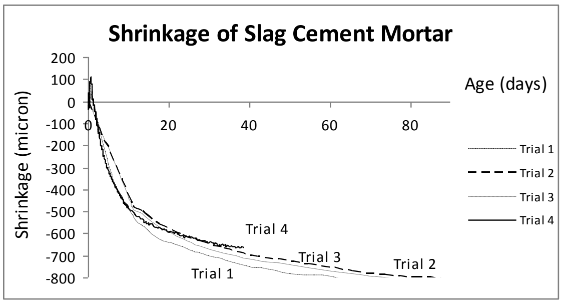

Fig 7 Reproducibility check on four measurements

(4) Relative humidity measurement

Specimens were prepared with the same size and mix proportion as listed in Table 4. The internal RH of specimens was measured according to previous proposed method [5] by using an embedded capacitive sensor covered by fabric pouch, as shown in Fig 8.

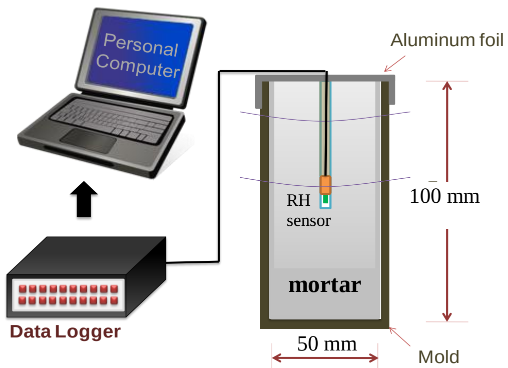

Fig 8 Internal relative humidity measurement

(5) Compression test

Compression test to obtain the strength of some specimens at 3, 7, and 28 days was conducted according to JIS A1108 [6]. An average from 3 identical specimens is determined for each variation. Each specimen having 50% of w/b was cured under sealed condition at a controlled condition chamber until loaded in compression at the specified age.

Some additional specimens for compression test were also prepared from some mortars. Specimens were made with mortar having 35% of water to binder ratio and the same curing condition as that for shrinkage specimens. Specimens were then loaded at 1, 3, 7, 14, and 28 days.

3. EXPERIMENTAL RESULTS AND DISCUSSION

3.1 Compression Test

Compressive strength of each slag cement mortar is plotted in Fig 9. Every specimens show a different compressive strength even the mix proportion and curing condition are the same. The highest early strength was given by specimen B while G shows the lowest strength rate.

According to research reported by Taylor [7], to insure higher early strength, usually cement containing a high amount of slag was produced with higher fineness. It also shows different pore structures in the matrix caused by different hydration mechanism resulted by variation of mineral compositions. Different mechanism causes variation value of strength development in slag cements mortar.

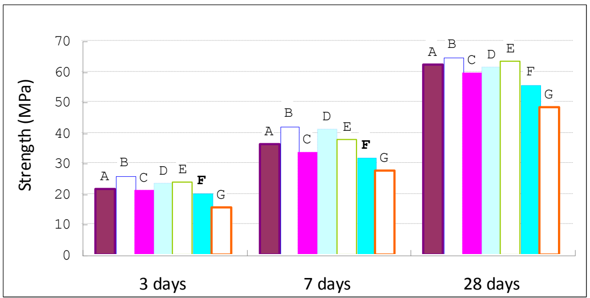

Fig 9 Compressive strength of slag cements A-G

3.2 Autogeneous shrinkage

(1) Cured at 20°C

The internal temperature curve of specimens is drawn in Fig 10. Specimen E shows the greatest internal temperature as a result of highest C_3A content. Specimens containing slag are observed to significantly reduce the maximum temperature achieved by that in OPC mortar during the early hydration. The variation of internal temperature shown by each specimen indicates different hydration process in the early age.

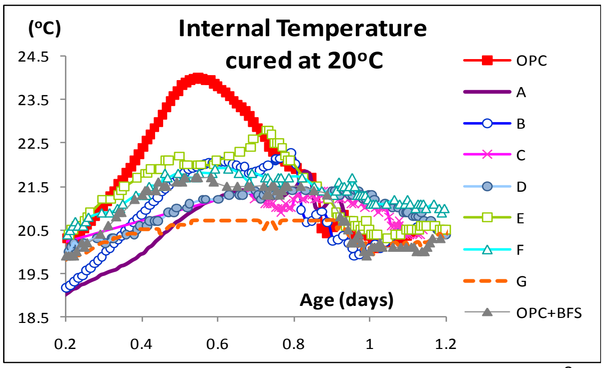

Fig 10 Internal temperature of specimens at 20°C

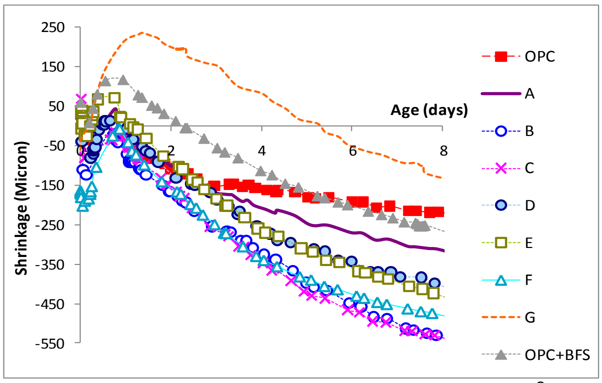

Fig 11 Mortar shrinkage 7days cured at 20°C

The autogeneous shrinkage curves of slag cements during the first week are represented in Fig 11.

It is interesting to recognize that gypsum content in slag cements leads to an increase of initial swelling of shrinkage just after casting. This swelling occurs at the beginning and then the strain decreases due to self-desiccation. This swelling deformation was also reported by Barcelo [8]. Specimen G has higher SO_3 and sulfate in the form of anhydrate which can control cement set. The effect of sulfate content promotes its expansion deformation at the early ages to obtain small shrinkage at later age.

Fig 12 shows the effect of exposure age on the shrinkage mortars cured at 20°C for 40 days. Introducing BFS as 40% of cement replacement leads higher shrinkage deformation as extended time.

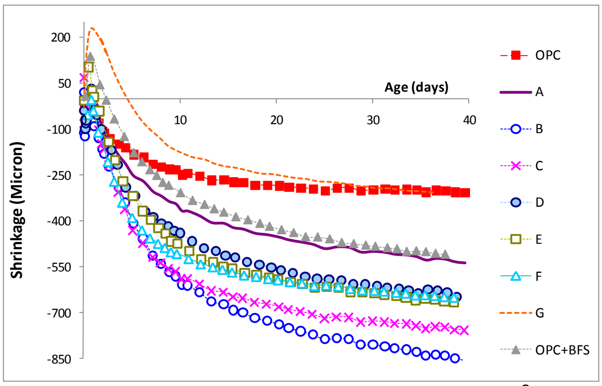

Fig 12 Shrinkage of specimens cured at 20°C for 40 days

There are some factors which affect the variation of the shrinkage values of slag cement type B. Physical and chemical properties play an important role.

Average particle size and particle width distribution (refer to Table 2) contribute a factor to lead greater shrinkage. The higher value N shows the more cement particle size becomes uniform. In this reason, specimen B, C, and E show higher shrinkage deformation as compared to other slag cement mortars.

Chemical content in slag cement is also one of the main factors to greater shrinkage. Calcite ($CaCO_3$) content, for an example, as shown in Table 3 is also thought to promote higher shrinkage deformation. Finally, specimen B has the highest amount of calcite and the most uniform size of particles showing the greatest shrinkage deformation. Specimen A does not have calcite content and has relatively broadened particle distribution. As a consequence, its shrinkage deformation is the smallest.

(2) Cured at 50°C

Internal temperature of some specimens cured at 50°C can be seen in Fig 13. Higher curing temperature shifts the peak of all internal temperatures and increases hydration rate rapidly.

The strain evolution cured at 50°C at early age is higher than that cured at 20°C as shown in Fig 14. The effect of higher temperature which can activate the shrinkage rate is more obvious for mortar G which contains higher BFS.

Fig 15 provides shrinkage deformation of slag cements. It may seem surprising to note that higher curing temperature does not lead autogeneous shrinkage magnitude for all slag cement type B, except specimen G. Except specimen G, specimen A, D, E, F, C, and B, are sorted in order of lower to higher shrinkage.

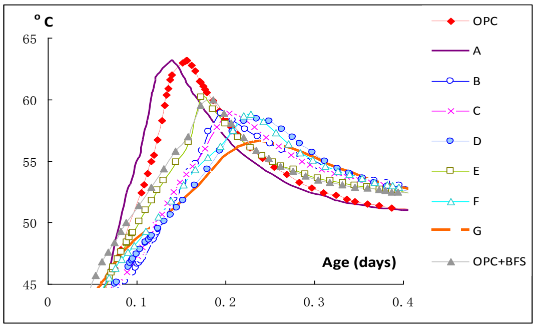

Fig 13 Internal temperature of mortars at 50°C

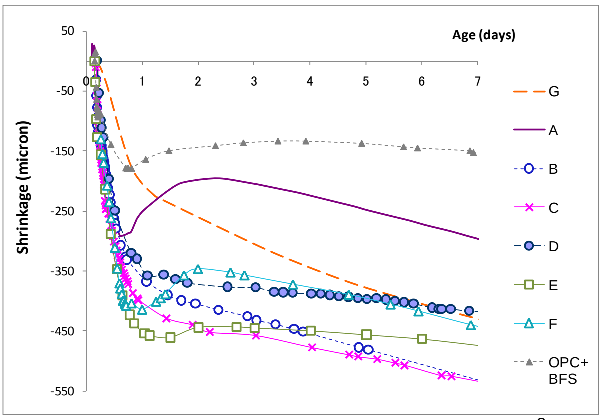

Fig 14 Mortar shrinkage 7days cured at 50°C

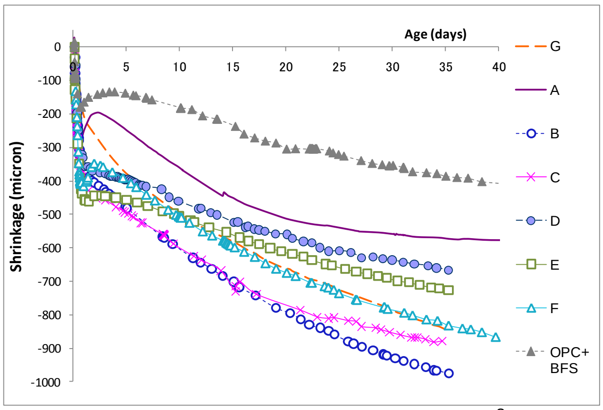

Fig 15 Shrinkage of specimen cured at 50°C for 40 days

Higher curing temperature affects only a rapid shrinkage rate at the first week due to increase of hydration. A very rapid shrinkage during the first day is followed by expansion at the following day and gradually decreases attributable to self-desiccation. A possible mechanism by this phenomenon can be explained as releasing of stress as a result of water in the ink-bottle spaces redistributed as condense water at higher temperature. Ishida [9] reported this water releasing which induced internal relative humidity rise at elevated temperature. This phenomenon was also have been shown by experimental work [5].

Then, it can be summarized that among all slag cements type B adopted in this study, there are three groups as compared to the control system: (a) the lowest shrinkage deformation which is shown by specimen A, (b) moderate deformation which is given by specimen D, E, F, and G, and finally (c) the greatest shrinkage, which is shown by specimen C and B.

3.2 Internal Relative Humidity

Specimens from low, moderate and high shrinkage deformation were prepared for internal RH measurement. The internal RH curves of some specimens are provided in Fig 16. Compared with OPC, the rate of RH decrease at slag cements shows rapid change at the very early age. This phenomenon was also reported at previous paper [5].

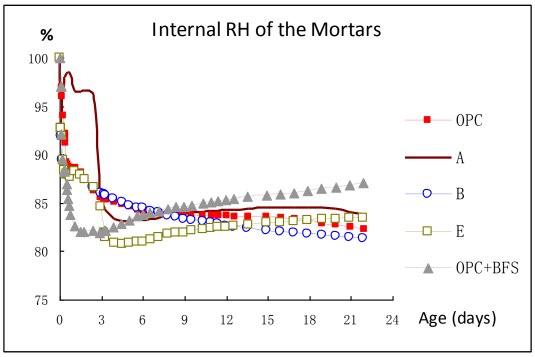

Fig 16 Relative humidity some specimens

Fineness of slag cement is considered as a mechanical accelerator. As the slag cement has finer particles consequence for larger surface area, it increases the water consumption and reduces pore sizes in cementitious matrix. This finer structure may induce the pores filled up which leads internal RH decreases abruptly due to self-desiccation.

3.3 Shrinkage and Strength Relation

Compressive strength of five specimens is plotted in Fig 17. In general, compressive strength development of slag cement specimens is OPC.

It was reported by Taylor [7] that replacement of 40% slag in the slag cement shows only 30-40% of reacted slag at 28 days. This may explain why compressive strength of slag cement mortars increases slower than OPC mortar.

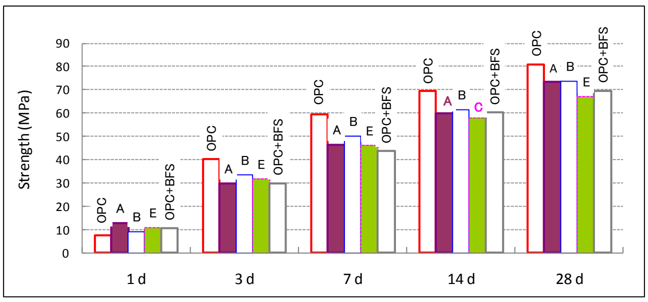

Fig 17 Compressive strength of some mortars

Fig 18 shows a relation between compressive strength and shrinkage at age 1d, 3d, 7d, 14d, and 28d. A linear relation is expressed by all specimens. The slope of control system is different from slag cement caused by less shrinkage deformation. When 40% BFS is introduced to the control system the slope changes to the same direction with other slag cements.

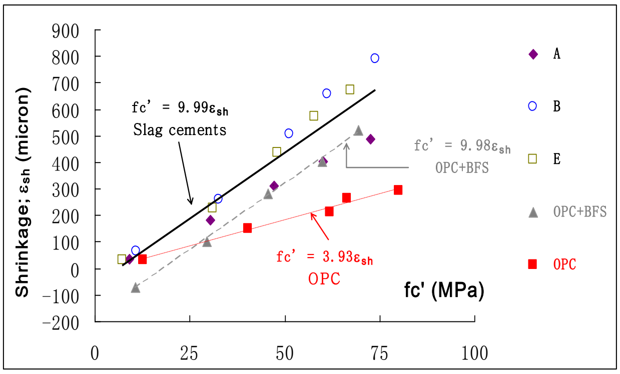

Fig 18 Relation between fc' and shrinkage of mortars at age 1d, 3d, 7d, 14d and 28d

It is evident that strength development at early age has a close relation with the porosity. The volume changes as solid formation from hydration products in the initial capillary space indicates the strength development. The characteristics of these hydration products are also represented by the type of the origin minerals of cement clinker. The more capillary space is occupied with the hydration products, the higher compressive strength will be achieved. This can also explain the different strength given by each specimen at the same age.

At the later ages, gradually the progression of hydration process generates finer gel pores form continuously. In case of this low water to binder ratio, self-desiccation occurs. Internal relative humidity in the capillary pores continues to decrease and then promote driving forces. The driving forces are believed to lead additional stress for shrinkage deformation. The slope presented by shrinkage-fc' relation at slag cement specimens is different from the slope of OPC specimens. The steeper slope of slag cement specimens indicates their different pore size caused by finer cement size particle, mineral content and chemical compound which are involved in the hydration process.

4. CONCLUSIONS

(1) At the exposure age, the rate of shrinkage deformation is still higher at slag cement type B result in greater deformation as compared to OPC which is almost constant at one week after casting.
(2) The mortars made with slag cement type B exhibited large variation of autogenous shrinkage. It may be due to creation of the early hydrated products, the greater chemical shrinkage, finer pore structure of the mortar containing BFS, and the particle shape of BFS. It is clear that this shrinkage mechanism cannot be only explained by the physical mechanism of self-desiccation induced by hydration
(3) The maximum shrinkage deformation in the slag cement mortars was about three times larger than that of the OPC mortar. It can be decreased by longer and proper curing of specimens at higher moisture condition, modifying the initial geometry of the cement particles and the minerals composition and also considering high replacement of cement part with BFS.
(4) Higher curing temperature affects a rapid shrinkage rate at the first day due to hydration increase, expansion at the following days and does not change the autogeneous shrinkage order for all slag cement type B at later ages.

ACKNOWLEDGEMENT

The authors would like to express their sincere thanks to the JSCE 333 committee supports and fruitful discussion from Prof. Toyoharu Nawa as the chairman of the committee. Deepest gratitude is also due to the Grant for Construction Technology Development by MILT for financial support to this research.

REFERENCES

[1] Tazawa, E. and Miyazawa, S., "Influence of Cement and Admixture on Autogeneous Shrinkage of Cement Paste," Cement and Concrete Research, vol.25 no.2, 1994, pp.281-287,
[2] JIS R 5211:2003, "Portland cement"
[3] Nito, N. et all, "Property Of Concrete using Portland Blast-Furnace Slag Cement B Class with Different Slag Grain and a Chemical Composition," JCA Proceedings of Cement & Concrete, no59, 2006, pp.231-238 (in Japanese)
[4] Nawa, T. and Horita, T., "Autogenous Shrinkage of High-Performance Concrete, Proceedings of the International Workshop on Microstructure and Durability to Predict Service Life of Concrete Structures," Sapporo, Japan, 2004
[5] Ekaputri, J. J. et all, "Internal Relative Humidity Measurement on Moisture Distribution of Mortar Considering Self-Dessication at Early Ages," JCI Annual Conference, vol 31 no 1, 2009, pp.643-648
[6] JIS A 1108:2006, "Method of Test for Compressive Strength of Concrete"
[7] Taylor H. F. W., "Cement Chemistry," Academic Press London, 1990, pp. 261-272
[8] Barcelo, L., Moranville, M. and Clavaud, B., "Autogenous Shrinkage of Concrete: a Balance between Autogenous Swelling and Self-desiccation," Cement and Concrete Research, 35, 2005, pp. 177-183
[9] Ishida, T., Maekawa, K. and Kishi, T., "Enhanced Modeling of Moisture Equilibrium and Transport in Cementitious Materials under Arbitrary Temperature and RH History," Cement and Concrete Research, vol. 37, 2007, pp. 565-578